Progress In Electromagnetics Research, Vol. 109, 475–491, 2010

NOVEL TWO-LAYER MILLIMETER-WAVE SLOT ARRAY ANTENNAS BASED ON SUBSTRATE INTEGRATED WAVEGUIDES

A. Bakhtafrooz and A. Borji

Department of Electrical and Computer Engineering
Isfahan University of Technology
Isfahan 84156-83111, Iran

D. Busuioc

DBC Group Inc.
P. O. Box 1001, Brookline, MA 02446, USA

S. Safavi-Naeini

Department of Electrical and Computer Engineering
University of Waterloo
Waterloo, Ontario, N2L 3G1, Canada

Abstract—A novel slot array antenna with two layers of substrate integrated waveguides (SIW) is presented for millimeter-wave wireless applications. Unlike conventional SIW-based slot arrays, in this structure a feed waveguide is placed underneath the main substrate layer containing the slot array and is coupled to the branches of the array via slanted slots. The proposed feeding structure results in a considerable reduction in size and eliminates unwanted radiations from the feed network. Experimental results for two slot arrays with 4×4 and 6×6 elements operating at 60 GHz are presented showing 14.8 dB and 18.5 dB gain, respectively. Furthermore, a novel doubly tapered transition between SIW and microstrip line is presented which is particularly useful in mm-wave applications.

Received 17 September 2010, Accepted 22 October 2010, Scheduled 6 November 2010
Corresponding author: Dan Busuioc (dbusuioc@uwaterloo.ca).

1. INTRODUCTION

Waveguide slot array antennas have received considerable attention in a variety of microwave and millimeter-wave applications where high performance antennas are required. Due to their high aperture efficiency, low side lobe levels, and low cross polarization, resonant slot arrays have found numerous applications in short range radars and millimeter-wave wireless systems such as collision avoidance radars [1], fixed wireless access (FWA) transceivers in K and Ka bands [2], mobile satellite terminals in Ku and Ka bands [3, 4], and broadBand home-link systems at 60 GHz [5]. Numerical simulation of waveguide slot arrays was recently addressed in [6]. Conventional resonant slot arrays can be very expensive due to high precision required in their manufacturing. Furthermore, because of using standard rectangular waveguides, the antenna array is thick and bulky and is not suitable for monolithic integration with planar microwave circuits.

Recently, the concept of substrate integrated waveguides (SIW) has enabled RF engineers to take advantage of low-loss transmission in rectangular waveguides within the printed circuit board [7]. Using SIWs has led to low profile, light weight, low cost, and compact microwave devices that are suitable for monolithic integration with printed circuits [8, 9]. In particular, a number of SIW-based slot array antennas have been reported in recent years [3, 10–12]. These arrays consist of one layer of dielectric substrate and are fed from one end through a coplanar feed network which significantly increases the size of the antenna. Furthermore, radiation from microstrip feed lines and junctions severely compromises the low side-lobe level of the slot array and increases cross polarization.

In this paper the design, fabrication, and characterization of a new slot array antenna with two layers of SIWs are presented. In the proposed structure which was briefly introduced by the authors in [13], the top substrate layer contains a parallel array of slotted SIWs that are short circuited at both ends, i.e., each SIW constitutes a linear slot array. Each branch of the slot array is excited through a slanted slot at its center etched on the common ground plane between the two layers. These coupling slots are fed through another waveguide which is perpendicular to the branches of the array and is integrated in the bottom substrate. The feed waveguide is excited by a microstrip line and the power is distributed to the branches of slot array through above center-inclined slots.

Two square arrays with 16 and 36 elements are designed, manufactured, and measured. Both arrays operate at 60 GHz and they show 14.8 dB and 18.5 dB of measured gain, respectively. Step by step

design procedure of the array antennas is discussed in Section 2 of this paper. Simulation and experimental results are presented in Section 3.

2. DESIGN PROCEDURE

The slot array is designed based on dielectric filled rectangular waveguides with solid walls. In the end, all waveguides will be replaced by equivalent SIWs. If the dimensions of SIWs are chosen carefully, no adjustments will be required for locations or dimensions of the slots. The design procedure of standard waveguide slot arrays was presented by Elliott in [14–16] and it is adopted here. Furthermore, the internal higher order mode coupling between adjacent slots was included in our design following the procedure given in [15].

2.1. Modeling Longitudinal Radiating Slot

The equivalent circuit of a longitudinal radiating slot is shown in Fig. 1. It consists of a shunt admittance for which a model must be developed in terms of frequency, slot length, and slot offset from the waveguide axis. To this end, a single slot is simulated by Ansoft HFSS as a two port network for a range of slot lengths, offsets, and frequencies. The reference plane is defined at the center of slot and the normalized admittance is extracted from scattering parameters. From the equivalent circuit we can write:

$$\frac{Y(x,l,f)}{G_0} = \frac{-2S_{11}}{1+S_{11}} = \frac{2(1-S_{21})}{S_{21}} \tag{1}$$

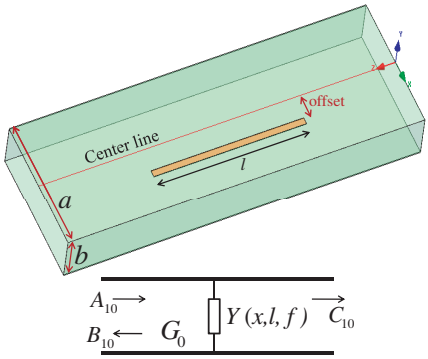

Figure 1. Circuit representation of longitudinal slot.

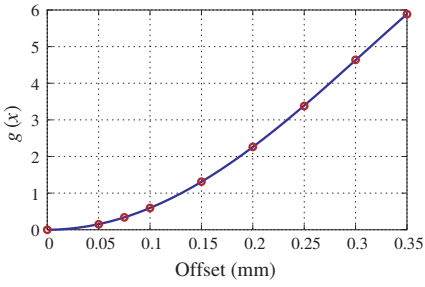

Figure 2. Normalized resonant conductance of single slot vs. offset $g(x)$.

in which G_0 is the characteristic admittance of the waveguide. As explained in [16, 17], the field on the slot is somewhat unsymmetrical and the above two formulas produce slightly different results, thus, their average value was used for slot admittance. In fact a more accurate equivalent circuit for the radiating slot is a T network which consists of two small series impedances on both sides of the shunt admittance [18]. The reason is that the amplitudes of forward and backward scattered waves from the slot are slightly different [17, 18], in other words S_{21} is not exactly equal to $1 + S_{11}$. However, in our work this asymmetry is negligible. Using the factorization proposed by Stegen and described in [17], we can write:

$$\frac{Y(x,l,f)}{G_0} = g(x)h(y) = g(x)\left[h_1(y) + jh_2(y)\right] \tag{2}$$

where x and l are the offset and length of slot, $g(x) = \Re\{Y(x,l,f_{\text{res}})\}/G_0$ is the normalized resonant conductance, $y = l/l_{\text{res}}$ is the ratio of length to resonant length and $h(y)$ is the ratio of normalized slot admittance to the resonant conductance. Obviously we must have $h_1(1) = 1$ and $h_2(1) = 0$. It has also been shown that the resonant length of a slot normalized to free space wavelength, denoted by $v(x) = 2\pi l_{\text{res}}/\lambda_0$, is only a function of slot offset. Therefore, calculation of the slot admittance which is a function of x, l and f is reduced to computation of three separate functions of a single variable, namely $g(x)$, $v(x)$, $h(y)$. Using the data obtained from parametric simulation of a single slot, a look up table is set up for the above three functions and cubic spline interpolation is used to calculate the normalized slot admittance for arbitrary dimensions during the array design procedure. Numerical results of these simulations are shown in Fig. 2 to Fig. 4. Furthermore, the directivity of a single resonant slot radiating into free space turns out to be 6.05 dB. In these simulations the width and height of the waveguide are 1.857 mm and 0.7874 mm, respectively. The material filling the waveguide is RT Duroid 5880 ($\epsilon_r = 2.2$) and the width of slot is $w = 0.1$ mm.

2.2. Modeling Slanted Coupling Slot

A common mechanism for feeding waveguide slot arrays is a center-inclined slot coupler shown in Fig. 5. Each coupling junction in slot array consists of a slanted coupling slot and a pair of longitudinal radiating slots located a quarter wavelength away in the branch line. This type of feed for conventional rectangular waveguide slot arrays has been extensively studied in the past [19–21]. Moreover, in [16] the design procedure for planar slot arrays using this type of feed is fully described. The amount of power coupled to the branch line is

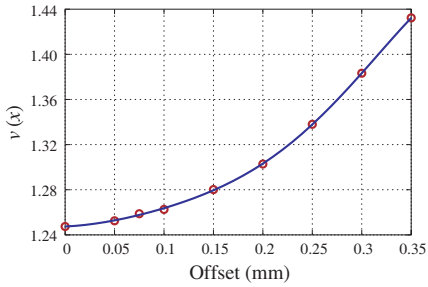

Figure 3. Normalized resonant length vs. offset $v(x) = k_0 l_{\text{res}}$.

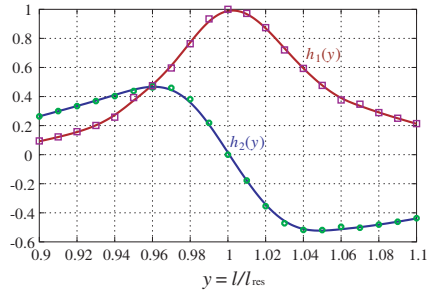

Figure 4. Shunt admittance of single slot normalized to resonant conductance $h(y) = h_1(y) + jh_2(y)$.

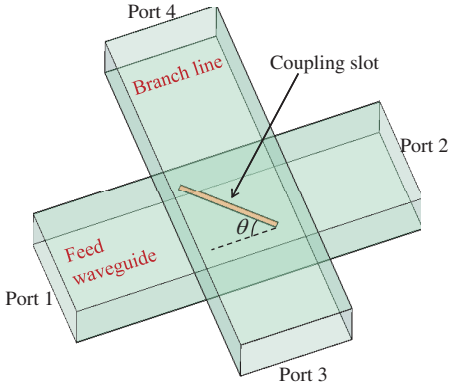

Figure 5. Center-inclined slot coupler.

controlled by the tilt angle θ (measured from the waveguide axis) and the length of coupling slot l_c which is usually selected to be resonant. The slanted slot acts as an impedance transformer between the feed waveguide in the bottom layer and the coupled branch on the top layer where the radiating slots are located. For a resonant slot, it has been shown in [16] that if Y^a is the total active admittance measured at quarter wavelength away from the center of coupling slot in the branch line and Z^a is the series load impedance that appears in the feed waveguide, then:

$$\frac{Z^a}{R_0} = \kappa^2 \frac{Y^a}{G_0} \tag{3}$$

$$\kappa^2 = \frac{S_{11}(\theta)}{1 - S_{11}(\theta)} \tag{4}$$

where κ is the coupling coefficient and S_{11} is the input scattering parameter of the slot coupler which is real because the slot is resonant. In order to build a model for the coupling junction which will be used in the array design procedure, the center-inclined slot coupler can be simulated in Ansoft HFSS for a range of tilt angles and the results for coupling coefficient and resonant length of slot can be tabulated and interpolated. In practice, however, it is possible to use a fixed tilt angle for all coupling slots even for non-uniform arrays and, therefore, no parametric modeling is necessary. In this case the correct voltage distribution is still achieved for branches of the array if the active admittance Y^a of each branch is selected properly instead of all being chosen equal [16]. This approach was adopted in the present work. It was shown in [20] that neglecting the higher-order mode coupling between the coupling slot and adjacent radiating slots may introduce significant errors in high performance antennas. This error can be corrected by adjusting the offset and length of radiating slots and tilt of the coupling slot based on the guidelines given in [20]. In our case numerical simulations of several linear arrays (single branch arrays) showed that for tilt angles less than about 10° the above higher order mode couplings are negligible and the input reflection coefficient of the array is as predicted by theory. Therefore no further adjustments of slot lengths and offsets were required.

2.3. Replacing Waveguides with Equivalent SIW

The structure of SIW is shown in Fig. 6 where p and d denote the period and diameter of via holes, respectively, and a is the physical width of SIW. Guided-wave characteristics of this structure have been extensively studied [22, 23]. In [23] a fairly accurate empirical formula with a relative error of less than 1% was presented for the equivalent width of a SIW. This equation was used here to calculate the physical width of SIW which produces the same propagation constant

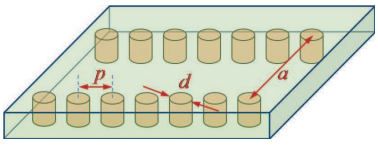

Figure 6. SIW structure

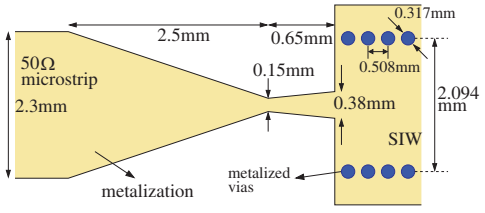

Figure 7. Doubly tapered transition between SIW and microstrip.

as a rectangular waveguide with solid walls. Interestingly, no further adjustment of slot locations and lengths were required after replacing the waveguides with SIW.

2.4. Microstrip to SIW Transition

A microstrip line is used to transfer the power to or from the antenna array. This transmission line is connected to the feed waveguide in the bottom layer. The transition between microstrip line and SIW is critical for achieving good impedance matching and small return loss. A tapered transition was proposed in [24] which is useful in most applications. However, in our design, the width of 50 Ω microstrip line is wider than the width of SIW and the proposed transition in [24] cannot be used. Therefore, a novel transition composed of two back-to-back tapered microstrip lines was designed and manually tuned in Ansoft HFSS to achieve impedance matching with low insertion loss. The layout of this transition is shown in Fig. 7 and final simulation results for its reflection and transmission coefficients are shown in Fig. 8. The insertion loss at 60 GHz is 1.035 dB.

3. SIMULATION AND MEASUREMENT RESULTS

3.1. Physical Parameters and Fabrication

Two square slot arrays, one with 4×4 elements and the other with 6×6 elements, were designed and fabricated. Both arrays have uniform slot voltage distribution and operate at 60 GHz. RT Duroid 5880 with dielectric constant of 2.2 was used for all substrate layers.

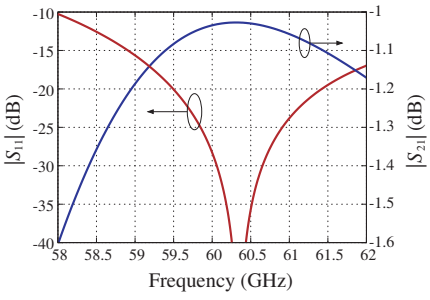

Figure 8. Magnitude of reflection and transmission coefficients of the new SIW-to-microstrip transition.

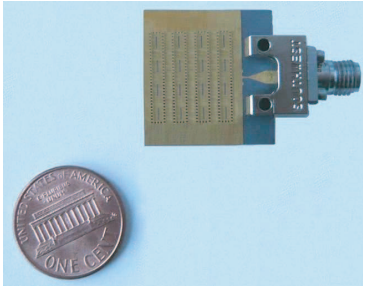

Figure 9. Fabricated 4×4 slot array.

Table 1. Parameters of coupling slots in both arrays.

array size	Length (l_c)	Tilt (θ)
4×4	1.770 mm	8°
6×6	1.784 mm	6°

The thickness of substrate was $b = 0.7874$ mm and that of the metal cladding was 17 µm. The spacing and the diameter of metallic vias were $p = 0.508$ mm and $d = 0.3175$ mm, respectively, and the width of all slots was $w = 0.1$ mm.

In order to maximize the gain, the spacing between adjacent slots is selected to be $0.8\lambda_0$ (λ_0 is the free space wavelength) or 4 mm at 60 GHz, thus, the guide wavelength at 60 GHz has to be 8 mm because the slots are $\lambda_g/2$ apart. This guide wavelength corresponds to the cut-off frequency of 54.42 GHz for the equivalent dielectric filled rectangular waveguide. Based on this cut-off frequency, the width of equivalent rectangular waveguide must be 1.857 mm which corresponds to the physical width of $a = 2.094$ mm for SIW according to the empirical formula given in [23]. Tilt angles and lengths of all slanted coupling slots were identical in each array and they are given in Table 1 for both antennas. Note that coupling slots are designed to be resonant at 60 GHz.

Two-sided printed circuit boards (PCB) were used to fabricate the top and bottom layers separately. For the top layer, radiating and coupling slots were etched on both sides of the PCB and metalized through holes were used to implement SIWs. In the bottom layer, coupling slots were etched on the top metal plane and the two PCBs were attached together using silver epoxy. In this process no blind vias are necessary which is a great practical advantage, however, precise alignment of the coupling slots is required. To save space, only the picture of fabricated 4×4 element array is shown in Fig. 9. The drawing of 6×6 element array is also shown in Fig. 10 which clearly shows the arrangement of all radiating and coupling slots. The locations and lengths of radiating slots in 4×4 array are given in Tables 2 and 3, respectively. Similarly data for 6×6 array is not presented here to save space. The total size of the slot array measured between opposite corners of the first and last branch waveguides is 14 mm × 16 mm for 4×4 array and 22 mm × 24 mm for 6×6 array. The size of radiating aperture measured between centers of the first and last radiating slots, located on opposite corners of the array, are 12.25 mm × 12 mm for 4×4 array and 20.3 mm × 20 mm for 6×6 array.

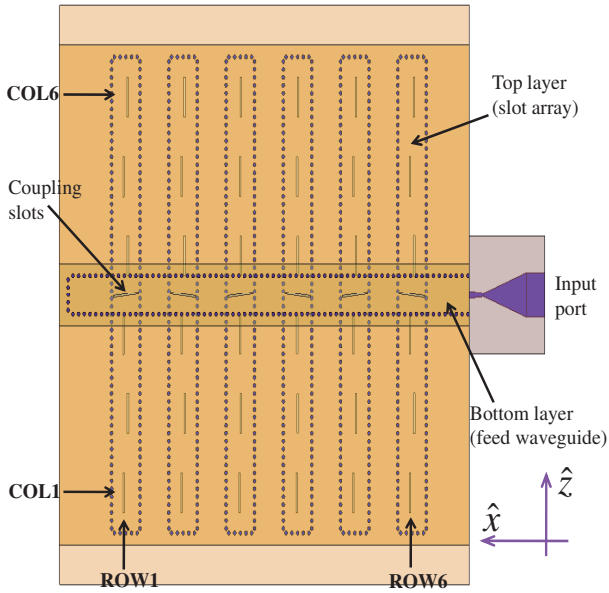

Figure 10. Picture of 6×6 array showing all radiating and coupling slots and input transition.

Table 2. Slot offsets in mm for 4×4 array.

x_{mn}	COL1	COL2	COL3	COL4
ROW1	+0.128	−0.110	+0.105	−0.131
ROW2	+0.083	−0.091	+0.083	−0.093
ROW3	+0.093	−0.083	+0.091	−0.083
ROW4	+0.131	−0.105	+0.110	−0.128

Table 3. Slot lengths in mm for 4×4 array.

l_{mn}	COL1	COL2	COL3	COL4
ROW1	2.038	2.026	2.032	2.032
ROW2	1.984	1.972	1.978	1.982
ROW3	1.982	1.978	1.972	1.984
ROW4	2.032	2.032	2.026	2.038

3.2. EM Simulation Setup

An important parameter in electromagnetic simulation of antennas and circuits at very high frequencies is the loss tangent of dielectric materials used in the structure. In order to obtain a correct estimation of dissipative losses, it is critical to use accurate values of loss tangents at frequencies of interest. Measured loss tangent and dielectric constant of RT Duroid 5880 and several other substrate materials by Rogers Corp. over the frequency band of 1–50 GHz were reported in [25]. In particular, the following equation was given in [25] which closely approximates the measured loss tangent of RT Duroid 5880 from 5 GHz to 50 GHz:

$$\tan\delta = 0.000008f + 0.0005 \tag{5}$$

in which f is frequency in GHz. Consequently, it would be reasonable to assume that the loss tangent at 60 GHz must be very close to 0.001 and this value was used in all HFSS simulations. All numerical simulations were performed using actual SIWs, i.e., with via walls. However, which is present in all measurements was not included in HFSS simulations, i.e., the structure was excited directly at 50 Ω microstrip line using a waveguide port. Furthermore, the entire array was placed inside a rectangular box with radiation boundary conditions so as to take the effect of finite ground plane into account.

3.3. Return Loss

Measured and simulated reflection coefficients of the two slot arrays are shown in Fig. 11 and Fig. 12. The discrepancy between measurements and simulations is caused by a number of factors. Poor calibration of the network analyzer and exclusion of the input connector in EM simulations substantially contribute to the discrepancies specially for S_{11}. Any mismatch between the connector and microstrip line, which could be due to poor quality of soldering, can also have a significant impact on the measured return loss.

There are also two major degrading factors, both related to the manufacturing process, that greatly affect the reflection coefficient and the gain of two layer slot arrays. One is the thickness of silver epoxy used to attach the two layers which was not accounted for in the design of slot arrays and the other is the slight misalignment between the top and bottom layers when they are glued together. A fairly thorough parametric study was carried out to determine the effect of above issues on the antenna performance and a summary of the results are presented in the following.

During the design of center-inclined coupling slots the thickness of middle ground plane was assumed to be twice the thickness of copper

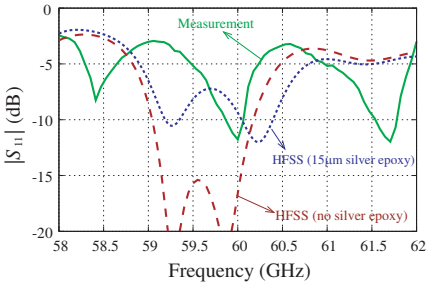

Figure 11. Measured and simulated S_{11} for 4×4 array including the effect of 15 μm silver epoxy layer added between the two PCB layers.

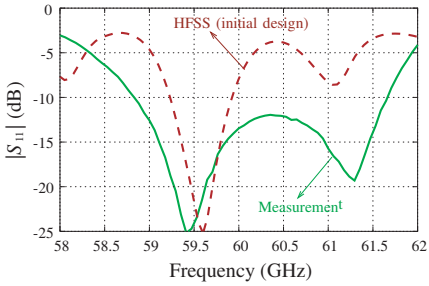

Figure 12. Measured and simulated S_{11} for 6×6 array.

cladding of PCB boards, namely $2 \times 17\,\mu m = 34\,\mu m$. This was used for the design of arrays and initial simulations of antennas, however, in practice the silver epoxy adds to the actual thickness of coupling slots. Further simulations showed that increasing the thickness of coupling slots had a significant effect on the coupling coefficient of slanted slot couplers which, in turn, had a considerable impact on the input reflection coefficient. Typical behavior of magnitude and phase of coupling coefficient in terms of the thickness of coupling slot is shown in Fig. 13 and Fig. 14. In our design the value of κ at thickness of 34 μm was used which is a real number because the coupling slot is resonant. However, in practice the actual thickness is larger due to the silver epoxy and the realized coupling coefficient is different.

In order to investigate the effect of increased thickness in coupling slots on the performance of antenna array, the 4×4 array was simulated in HFSS with 15–25 μm of extra thickness added to the ground plane separating the two layers, i.e., the actual thickness of coupling slots was considered to be 49–59 μm. The typical result of this simulation for the input reflection coefficient is shown in Fig. 11 along with the original simulation results. Clearly the added thickness of silver epoxy significantly affects the return loss and it must be considered during the design process. It must be mentioned that the return loss decreases further as the epoxy layer becomes thicker. The effect of this extra thickness on the gain will be discussed in the following sub-section.

The other issue is the misalignment between the top and bottom layers when they are attached together. Any offset caused by manufacturing tolerances directly affects the width and length of coupling slots which, in turn, has a significant impact on the return

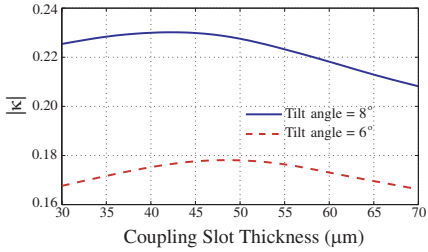

Figure 13. Magnitude of coupling coefficient for slot coupler.

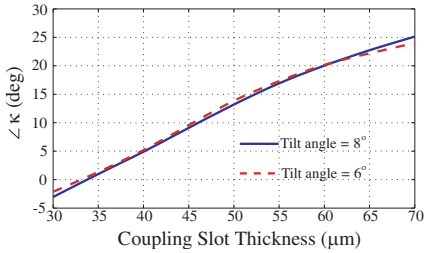

Figure 14. Phase of coupling coefficient for slot coupler.

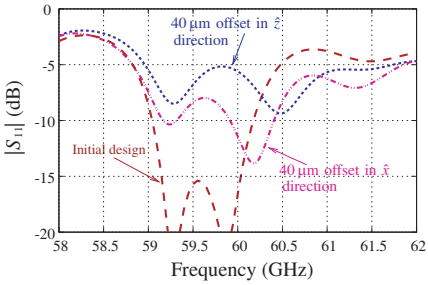

Figure 15. Simulated S_{11} for 4×4 array including the effect of 40 μm misalignment between the top and bottom layers. The two principal directions are shown in Fig. 10.

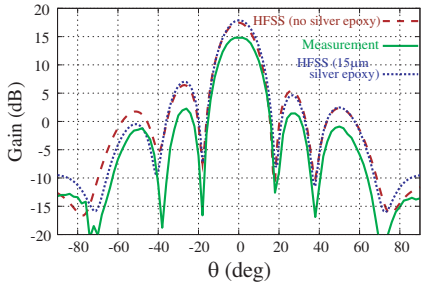

Figure 16. H-plane gain of the 4×4 array at 60 GHz including the effect of 15 μm silver epoxy layer added between the two PCB layers.

loss and gain. The 4×4 array was simulated with different values of misalignment (or offset) between the two layers and typical results for input reflection coefficient are shown in Fig. 15. Note that two types of offsets were considered: one in which the misalignment was assumed to be in $\hat{x}$ direction (perpendicular to the radiating slots) and in the other it was assumed to be in $\hat{z}$ direction (parallel to the radiating slots). These principal directions are shown in Fig. 10. Obviously the unwanted offset between the two layers deteriorates the reflection coefficient. The effect of this misalignment on the gain will be discussed in the following sub-section.

3.4. Radiation Pattern and Gain

The gain of the 4×4 array at 60 GHz in two principal planes is shown in Fig. 16 and Fig. 17. In addition to the measured and original simulation

data with no silver epoxy between the two PCB layers, the results of simulation with added thickness of coupling slots are also reported. It must be emphasized that the simulated gain is referenced to the power *accepted* at the input port of the antenna while the measured gain is referenced to the *incident* power (usually called realized gain). In other words, one has to divide the realized gain by $1 - |S_{11}|^2$ to obtain the gain. In Table 4 the gain and realized gain of the 4×4 array for different thicknesses of epoxy layer are compared. It is interesting to note that by adding the extra layer of metal the *gain* increases a little bit but the

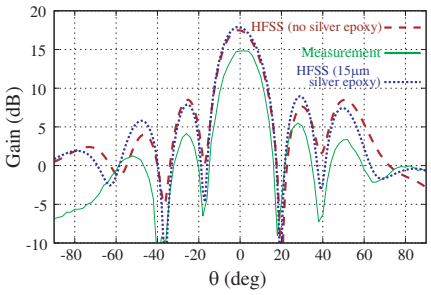

Figure 17. *E*-plane gain of the 4×4 array at 60 GHz including the effect of 15 μm silver epoxy layer added between the two PCB layers.

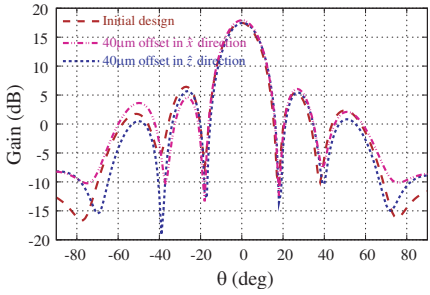

Figure 18. *H*-plane *gain* of the 4×4 array at 60 GHz including the effect of 40 μm misalignment between the layers.

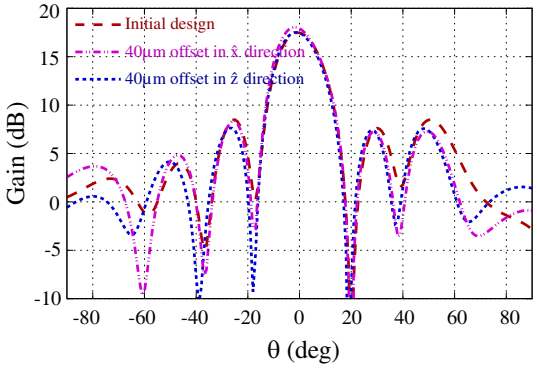

Figure 19. *E*-plane *gain* of the 4×4 array at 60 GHz including the effect of 40 μm misalignment between the layers.

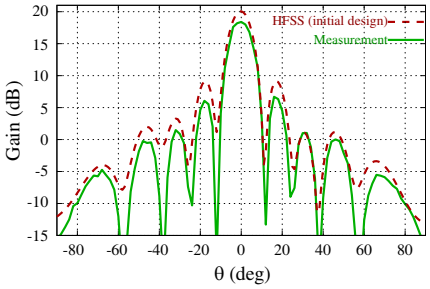

Figure 20. *H*-plane *gain* of the 6×6 array at 60 GHz.

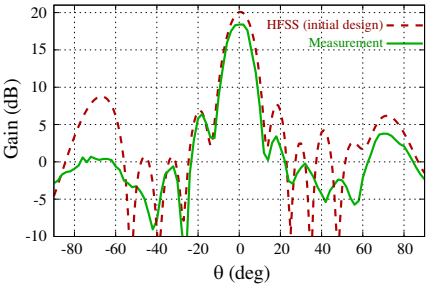

Figure 21. *E*-plane *gain* of the 6×6 array at 60 GHz.

Table 4. Gain of 4×4 array vs. the thickness of silver epoxy inserted between the two layers.

	Measured	Simulation			
		Initial design	15 µm epoxy	20 µm epoxy	25 µm epoxy
Gain	15.1	17.47	17.88	17.81	17.63
Realized Gain	14.8	17.37	17.35	16.71	16.07

Table 5. Simulated gain of 4×4 array vs. manufacturing offsets (misalignment) between the two layers.

	Initial design	40 µm in $\hat{z}$ direction	40 µm in $\hat{x}$ direction	50 µm in $\hat{z}$ direction	50 µm in $\hat{x}$ direction
Gain	17.47	17.45	17.91	16.76	17.82
Realized Gain	17.37	16.06	17.59	14.36	17.23

realized gain drops rapidly because of the large reflection at input port. The effect of misalignment between the two layers on antenna gain is illustrated in Fig. 18 and Fig. 19 where a 40 µm offset between the two layers was considered. Furthermore, in Table 5 the values of gain and realized gain for two sets of misalignments are compared. Note that the misalignment has little effect on the gain but substantially affects the realized gain because of poor return loss.

Finally, the *gain* of the 6×6 array in two principal planes are shown

in Fig. 20 and Fig. 21. The measured gain and reflection coefficient of this array at 60 GHz were 18.4 dB and −13.46 dB, respectively, which translates into a gain of 18.6 dB. Its simulated gain, however, is 20.06 dB. Considering the fact that a fairly accurate value for the loss tangent of substrate material was used in simulations and taking the previously discussed manufacturing issues into consideration, it seems that the above disagreements between measured and simulated gain of both antenna arrays could be mainly due to poor calibration and possibly slight misalignment in the measurement setup.

4. CONCLUSION

A new configuration for substrate integrated slot arrays was proposed and two millimeter-wave antennas were designed and manufactured. The new design eliminates the corporate microstrip feed network and enhances aperture efficiency by employing another integrated waveguide underneath the slot array which distributes the power to the branches of the array via center-inclined slots on the common ground plane. Furthermore, a new transition between microstrip line and SIW was proposed which is particularly useful in millimeter-wave applications where the waveguide width is small. The new antennas are very compact and are useful for a variety of 60 GHz applications, particularly, for ultra high-speed wireless networks and short range millimeter-wave radars.

ACKNOWLEDGMENT

Antenna arrays were manufactured by Polyflon company, Norwalk, CT, and all measurements were carried out by BTP Systems in Ludlow, MA.

REFERENCES

1. Hirokawa, J. and M. Ando, "76 GHz post-wall waveguide-fed parallel plate slot arrays for car-radar applications," *IEEE AP-S Int. Symp.*, Vol. 1, 98–101, 2000.
2. Kimura, Y., et al., "A low-cost and very compact wireless terminal integrated on the back of a waveguide planar array for 26 GHz band FWA systems," *IEEE Trans. Antennas Propagat.*, Vol. 53, No. 8, 2456–2462, Aug. 2005.
3. Yang, S., S. H. Suleiman, and A. E. Fathy, "Ku-band slot array

antennas for low profile mobile DBS applications: Printed vs. machined," *IEEE AP-S Int. Symp.*, 3137–3140, 2006.

4. Vincenti Gatti, R. and R. Sorrentino, "A Ka-band active scanning array for mobile satellite terminals using slotted waveguide technology," *25th Antenna Workshop on Satellite Antenna Technology*, Noordwijk, The Netherlands, Sep. 2002.
5. Nakano, H., et al., "Cost effective 60 GHz modules with a post-wall planar antenna for gigabit home-link system," *Proc. 33rd European Microwave Conference*, 891–894, 2003.
6. Hua, Y. and J.-Y. Li, "Analysis of longitudinal shunt waveguide slots using FEBI," *Journal of Electromagnetic Waves and Applications*, Vol. 23, No. 14–15, 2041–2046, 2009.
7. Deslandes, D. and K. Wu, "Single-substrate integration technique of planar circuits and waveguide filters," *IEEE Trans. Microwave Theory Tech.*, Vol. 51, No. 2, 593–596, Feb. 2003.
8. Wang, R., L.-S. Wu, and X.-L. Zhou, "Compact folded substrate integrated waveguide cavities and bandpass filter," *Progress In Electromagnetic Research*, Vol. 84, 135–147, 2008.
9. Li, R., X. Tang, and F. Xiao, "A novel substrate integrated waveguide square cavity dual-mode filter," *Journal of Electromagnetic Waves and Applications*, Vol. 23, No. 17–18, 2523–2529, 2009.
10. Lee, S., S. Yang, A. E. Fathy, and A. Elsherbini, "Development of a novel UWB vivaldi antenna array using SIW technology," *Progress In Electromagnetic Research*, Vol. 90, 369–384, 2009.
11. Yan, L., W. Hong, G. Hua, J. Chen, K. Wu, and T. J. Cui, "Simulation and experiment on SIW slot array antennas," *IEEE Microwave Wireless Comp. Letters*, Vol. 14, No. 9, 446–448, Sep. 2004.
12. Cheng, S., H. Yousef, and H. Kratz, "79 GHz slot antennas based on substrate integrated waveguides (SIW) in a flexible printed circuit board," *IEEE Trans. Antennas Propagat.*, Vol. 57, No. 1, 64–70, Jan. 2009.
13. Bakhtafrooz, A., A. Borji, D. Busuioc, and S. Safavi-Naeini, "Compact two-layer slot array antenna with SIW for 60 GHz wireless applications," *IEEE AP-S Int. Symp.*, 1–4, Jun. 2009.
14. Elliott, R. S., "An improved design procedure for small arrays of shunt slots," *IEEE Trans. Antennas Propagat.*, Vol. 31, No. 1, 48–53, Jan. 1983.
15. Elliott, R. S. and W. R. O'Loughlin, "The design of slot arrays including internal mutual coupling," *IEEE Trans. Antennas Propagat.*, Vol. 34, No. 9, 1149–1154, Sep. 1986.

16. Elliot, R. S., "The design of waveguide-fed slot arrays," *Antenna Handbook*, Y. T. Lo and S. W. Lee (eds.), Chap. 12, Van Nostrand Reinhold, New York, 1993.
17. Stern, G. J. and R. S. Elliott, "Resonant length of longitudinal slots and validity of circuit representation: Theory and experiment," *IEEE Trans. Antennas Propagat.*, Vol. 33, No. 11, 1264–1271, Nov. 1985.
18. Coetzee, J. C. and J. Joubert, "Analysis procedure for arrays of waveguide slot doublets based on the full T-netwrok equivalent circuit representaion of radiators," *IEE Proc. Microw. Antennas Propag.*, Vol. 147, No. 3, 173–178, Jun. 2000.
19. Rengarajan, S. R., "Analysis of a center-inclined waveguide slot coupler," *IEEE Trans. Microwave Theory Tech.*, Vol. 37, No. 5, 884–889, May 1989.
20. Rengarajan, S. R. and G. M. Shaw, "Accurate characterization of coupling junctions in waveguide-fed planar slot arrays," *IEEE Trans. Microwave Theory Tech.*, Vol. 42, No. 12, 2239–2248, Dec. 1994.
21. Rengarajan, S. R., "Higher order mode coupling effects in the feeding waveguide of a planar slot array," *IEEE Trans. Microwave Theory Tech.*, Vol. 39, No. 7, 1219–1223, Jul. 1991.
22. Xu, F. and K. Wu, "Guided-wave and leakage characteristics of substrate integrated waveguide," *IEEE Trans. Microwave Theory Tech.*, Vol. 53, No. 1, 66–72, Jan. 2005.
23. Yan, L., W. Hong, K. Wu, and T. J. Cui, "Investigations of the propagation characteristics of the substrate integrated waveguide based on the method of lines," *IEE Proceedings — Microwaves, Antennas and Propagation*, Vol. 152, No. 1, 35–42, Feb. 2005.
24. Deslandes, D. and K. Wu, "Integrated microstrip and rectangular waveguide in planar form," *IEEE Microwave Wireless Comp. Letters*, Vol. 11, No. 2, 68–70, Feb. 2001.
25. Horn, A., "Dielectric constant and loss of selected grades of Rogers high frequency circuit substrates from 1–50 GHz," Tech. Rep. 5788, Rogers Corp., Rogers, CT, Sep. 2003.